Energy Conversion and Management: X 20 (2023) 100480

Contents lists available at ScienceDirect

Energy Conversion and Management: X

journal homepage: www.sciencedirect.com/journal/energy-conversion-and-management-x

Dynamic simulation of a 4th generation district heating network with the presence of prosumers

T. Testasecca *, P. Catrini, M. Beccali, A. Piacentino

Department of Engineering, University of Palermo, Palermo, Italy

ARTICLE INFO

Keywords:
Energy savings
Renewable energy
District heating
Prosumer
Dynamic modelling
Ring network

ABSTRACT

District Heating Network is identified as a promising technology for decarbonizing urban areas. Thanks to the surplus of heat available from distributed renewable energy plants, a typical heat consumer of the network could become an energy producer during the day (typically referred to as a "prosumer"). Most of the models for thermal grids developed during past years usually assumed a centralized production of the consumed heat. The increasing presence of prosumers will require accurate dynamic modelling to monitor the changes induced in the thermohydraulic parameters of the network. To fill this knowledge gap, this paper aims at developing a model of a thermal grid with prosumers in the TRNSYS environment. The model allows for the dynamic monitoring of the main thermohydraulic parameters of the network. To show these capabilities, a ring-shaped network serving a cluster of 10 residential users located in Palermo (Italy) was assumed as the case study. Different scenarios are investigated based on the presence of solar collectors, prosumers along the network, and cooling by an absorption chiller. The achievable energy and emissions savings are calculated. The results of the study show that even only decreasing the operating temperature can significantly reduce heat losses via the network pipes. In particular, a temperature drop from 100 °C to 80 °C can reduce heat losses by 27.1%. Furthermore, the heat losses can be decreased by up to 52.8% when the network temperature is lowered from 100 °C to 60 °C. Additionally, the presence of prosumers and the solar field could lead to a 31.3% reduction in the energy produced by the centralized plant and a 17.6% reduction in energy consumed for pumping.

1. Introduction

To be in line with the goals of the European Green Deal [1], a synergy between building efficiency, integration of renewable energy sources (RES), and more efficient energy production systems is required. According to the "Heating" report by the International Energy Agency (IEA) [2], the share of ultra-low-carbon technologies in building heating systems needs to be urgently increased. Among the proposed technologies, district heating and cooling networks (DHC) play a key role in reducing the emissions of buildings. Since 2010, connections to District Heating Networks (DHNs) have increased by a factor of 3.5% per year, but further efforts are still needed to reduce emissions [2]. China, which is responsible for more than a quarter of global heat demand, has the fastest-growing DHN capacity in the world, and DHC networks in Europe meet more than 8% of total heat demand in countries such as Finland, Denmark, Sweden, and the Baltics [3]. In Italy, the technology is located only in the North, but its extension has quadrupled from 2000 to 2019 while the energy input has tripled [4]. Fossil fuels are still the dominant energy source, whereas RES (mainly biomass) provided less than 8% of the energy used [3]. Iceland has achieved nearly 100% renewables thanks to its geothermal resources and Denmark is leading the way in integrating solar thermal energy into District Heating (DH), accounting for more than three-quarters of the thermal installed capacity worldwide at the end of 2018 [3]. In Italy, in 2019, 16% of the energy fed into DH networks was provided by RES such as biomass and geothermal energy [4]. DHNs using large solar collector plants have been built in countries such as Denmark, China, Sweden, Saudi Arabia, and Austria for a total worldwide installed capacity of 1.6 GW_{th} [5].

From a technological point of view, during the decades, it has been observed a decrease in the level of operating temperature and pressure of DHNs, which led, in turn, to a reduction in heat losses (and therefore lower operating costs) and in pipe stress. In the literature, this evolution has been described by introducing the concept of " DHN generation" [6]. Almost all DHNs installed today belong to Generation 3rd [7]. These districts operate with pressurized water and temperatures between 80 °C and 100 °C. Generally, these systems are fed by large-scale centralized cogeneration plants (CHPs) with an emission factor of 150–300 g of

* Corresponding author.
E-mail address: tancredi.testasecca@unipa.it (T. Testasecca).

https://doi.org/10.1016/j.ecmx.2023.100480
Received 6 May 2023; Received in revised form 7 October 2023; Accepted 2 November 2023
Available online 6 November 2023

Nomenclature

c	[dimensionless], Contemporaneity factor
c_w	[kJ/kgK], Specific heat of water
D_i	[m], Diameter of the pipe in the branch *i*
ΔP	[bar], Pressure drop
ΔP_i	[bar], Pressure difference between the ends of the pipe in the branch *i*
$\Delta P_{s.i}$	[bar], Specific pressure drop in the branch *i*
ε_{pipe}	[m], Roughness of the pipe
η_{CHP}	[dimensionless], Efficiency of the cogenerator
f_{el}	[g/kWh], Conversion factor for carbon dioxide emission of the electricity
f_{NG}	[g/kWh], Conversion factor for carbon dioxide emission of the Natural Gas
h_i	[kJ/kg], Specific enthalpy of the inlet flow rate in node *j*
h_j	[kJ/kg], Specific enthalpy of the outlet flow rate in node *j*
L_i	[m], Length of the pipe in the branch *i*
LHV_{NG}	[kWh/kg], Lower heat value of the Natural Gas
λ_i	[dimensionless], Darcy friction factor in the branch *i*
$\dot{m}_{gen}$	[kg/s], Flow rate treated by the power plant
$\dot{m}_{in}$	[kg/s], Flow rate that enters the pipe
$\dot{m}_i$	[kg/s], Flow rate that enters the node *j*
$\dot{m}_j$	[kg/s], Flow rate that flows in the user *j*
$\dot{m}_o$	[kg/s], Flow rate that exits the node *j*
P_o*	[bar], Pressure just before supply-side pumps
P_o* R	[bar], Pressure just before return-side pumps
$\dot{Q}_{user:j}$	[kW], Thermal demand of the user in node *j*
$\dot{Q}_{cons:j}$	[kW], Demand of heat for domestic hot water or space heating/cooling by absorption chiller of the user in the node *j*
$\dot{Q}_{cons:SH:j}$	[kW], Demand of heat for space heating of the user in the node *j*
$\dot{Q}_{cons:ABS:j}$	[kW], Maximum heating demand for the absorption chiller in the node *j*
$\dot{Q}_{gen}$	[kW], Thermal power generated by the main power plant
$\dot{Q}_{losses}$	[kW], Overall heat losses in the network
$\dot{Q}_{pro:j}$	[kW], Thermal power produced by the producer in the node *j*
$\dot{Q}_{pros:j}$	[kW], Thermal power available from user prosumer in the node *j*
$\dot{Q}_{sto:j}$	[kW], Thermal power stored in the storage in the node j
$\dot{Q}_{stor:j}$	[kW], Thermal power stored of the user in the node j
ρ_i	[kg/m^3], Density of water in the branch *i*
Re_i	[dimensionless], Reynolds number in the branch *i*
T_o*	[°C], Temperature of the supply-side water at the end of the last branch
T_o* R	[°C], Temperature of water just before return-side pumps
T_s	[°C], Supply temperature
T_r	[°C], Return temperature
v_i	[m/s], Velocity of water in the branch *i*
W_{pump}	[kWh], Energy consumption of the pump

Acronyms

CCCP	Conventional Central Circulating Pump
CHP	Cogeneration Plant
CO_2	Carbon Dioxide
DH	District Heating
DHC	District Heating and Cooling Network
DHN	District Heating Network
DHW	Domestic Hot Water
DVSP	Distributed Variable Speed Pump
gCO_2	Grams of carbon dioxide
HP	Heat Pump
IEA	International Energy Agency
No.	Number
RES	Renewable Energy Sources
SH	Space Heating
y	Yearly

carbon dioxide (CO_2) for thermal kWh [2]. A decrease in network temperature can not only reduce heat loss but would facilitate the use of RES such as solar, geothermal, and waste heat from industrial processes, data centres, and supermarkets. In this respect, 4th and 5th generation DHNs are currently being investigated. In particular, 4th generation DHNs operate at maximum temperatures between 60 °C and 70 °C and they are often combined with users whose heating system works at medium–low temperatures. This operating temperature would allow the integration of RES and, additionally, the CHP will produce heat more efficiently [6]. Sorknæs et al. [8] proved that, for a 4th generation DHN, grid losses and total annual energy system costs decrease while the efficiency of the heat generation systems increases compared to the 3rd generation base case.

Seasonal storage systems such as Aquifer Thermal Energy Storage could provide flexibility to the entire system by storing heat in summer for use in winter and vice versa [9]. In the framework of 4th generation DHNs, the figure of the "prosumer" has been introduced [10]. A prosumer is a a typical heat consumer that could become a decentralized producer thanks to exceeding heat produced on-site by RES. For instance, a house equipped with solar thermal panels that, at a time of low self-consumption, could transfer the surplus heat to the grid, used by a neighbouring user. It is also possible to use the surplus of electricity available from the grid in contexts of high-RES penetration, to feed "Power to Heat" technologies such as heat pumps (HPs) to supply heat into the grid. In such a scenario, there would be an integration between the electricity and heat grids, in which the HPs would contribute to reducing the imbalance between production and demand on the electricity grid in the event of high penetration of RES, with benefits for the control of the electricity grid itself [11]. This principle is the basis for Smart Energy Systems (conceived as an evolution of the Smart Energy Grid) in which the electricity, heat, and gas grids will be able to interact with each other. Finally, 5th gen. networks represent a technology that should not replace Generation IV networks but complement them [6]. In these, a layout of a single-loop network with water at a temperature between 20 °C and 30 °C is often assumed. This temperature level would make heat loss negligible and accept any heat source available in the system. However, booster HPs should be installed at each user to obtain water at the required temperature level. This system can guarantee the simultaneous production of cooling and domestic hot water (DHW) without requiring a 4-pipe system to carry hot and cold water at the same moment.

In a context where heat generation becomes distributed, the impact of prosumers on the operation of DHN must be evaluated. Gross et al. [12] developed a tool for modelling 4th and 5th-generation DHN including prosumers, based on graph theories by Hardy-Cross and Wallenten. For a case study, the authors estimated a reduction in thermal losses of 5th Gen. case by more than 80% than the 4th Gen. case, and in both cases, the prosumers covered about 18.7% of the total heating energy. Brand et al. [13] showed that the presence of prosumers highly affects the temperature of the supply network, the velocity of water, and the differential pressure at each node. Abokersh et al. [14] analyzed the economic feasibility of a hypothetical solar-assisted DHN with HPs in a small neighbourhood in Madrid coupling a TRNSYS (TRaNsient System

Simulation tool [15]) model and a multi-objective optimization by an artificial neural network. Compared to traditional boiler production, in their case study, it was possible to reduce the environmental impact by 82.5% with a payback period of 26 years. The study presented by Hmadi et al. [16] proved that also in a desert climate a solar thermal DHC would reduce the annual electrical consumption by a factor of 5.8 compared to conventional district thermal plants. To calculate the optimum surface of collectors and storage volume, simulations were made on integrating an optimization program.

Due to the European Union interest in increasing e-mobility, the number of electric vehicles is increasing and thus, new opportunities for the development of smart energy systems could arise. In this respect, Calise et al. modelled a smart grid with a small DHN on TRNSYS to analyze the impact of electric vehicles in the system demonstrating that with an accurate charging strategy, it is possible to reach energy and cost savings [17]. In the framework of integration between smart grids and DHNs, a 5th generation bidirectional heating/cooling network was designed and modelled in TRNSYS for a 50-building district in Leganés (Spain) [18]. The network uses water-to-water HPs, ground HPs, and a photovoltaic field achieving up to 64% primary energy saving index with a payback period of 33 years. While the results are indeed promising, it is important to note that prosumers are not considered and the work lacks of a comprehensive analysis on the hourly trend of hydraulic variables such as flow rate and pressures in the branches of the network.

The ring topology is typically adopted in fourth and fifth-generation networks since it facilitates interaction with prosumers. The challenges, such as increased heat losses in the final pipe of the ring, are mitigated by the lower operating temperature. In this context, contemporary research is exploring new methodologies for optimizing the topology of fourth and fifth-generation DHNs [19]. Instances of the application of ring-shaped networks, where CHPs are supported by waste heat from datacentres, are documented in [20].

Regarding the hydraulic behaviour of DHNs with different heat sources, different studies and methodologies were presented in these years. Augusto et al. [21] proposed a methodology, based on the Newton-Rhapson method, for establishing an optimal design for a district cooling system with a looped network. Eremin et al. [22] presented a study where Kirchhoff's laws are applied in a multi-ring branched DHN with two heat sources, and, using iterative calculation methods, they reduced the computation costs. Worth noting that Kirchhoff's laws are also used in a quasi-steady state model of a DHN to compare distributed variable speed pumps (DVSP) instead of conventional central circulating pumps (CCCP) [23]. Considering flow rates, pump heads, and transportation power consumptions the authors demonstrated that using DVSP could achieve electricity saving of up to 71% and it could be also applied to hydraulic predictions. In the same way, Wang et al. [24] proposed a new method for the hydraulic regulation of DVSP in a DHN which could adapt efficiently the flow rates in all scenarios. In the theoretical multi-source DHN they considered, in comparison with CCCP they achieved an energy saving up to 90.3%. For investigating the relationship between control variables and thermohydraulic behaviour in steady state, the authors in [25] developed a mathematical model for a DHN with prosumers.

This brief state-of-art proved that studies on the dynamic behaviour of all the main physical variables in DHC appear to be few or fragmentary, for this reason, a better understanding is needed to facilitate the development of new generations of DHNs with the presence of prosumers. As a matter of fact, it is interesting and necessary to analyse how temperatures, flow rates, and pressures are affected when a prosumer injects heat into the network while accounting for dynamic aspects like the thermal inertia of the DHN. In this regard, the scope of this paper is to build a dynamic model for a DHN that allows for obtaining more realistic results for the operation of a 3rd and 4th generation network with the inclusion of multiple heat sources of RES. The object of this paper is innovative because it could help to fulfil the lack of information on the thermohydraulic behaviour of a grid operating with many prosumers, whose presence influences the grid itself and makes it necessary to approach differently the design and the operation. Thanks to the focus on the pressure values, it is possible to notice the way the power of the main pumps will change when a prosumer pumps hot water in the supply loop. A double loop ring-shaped network is modelled in TRNSYS environment to perform dynamic analysis and to monitor the thermohydraulic variables in multiple conditions of operation. The preliminary design phase aims at sizing the pipe diameters, choosing the units to be used in the thermal power station, and choosing the pump by studying the pressure drops in the circuit. Different scenarios are investigated according to the temperature of the network and the number and type of prosumers.

2. Methods and materials

To ensure the self-consistency of this work, the main equations used to describe the thermal–hydraulic behaviour of a DHN are first detailed. Then, the TRNSYS model of the case study is presented. It is worth noting that the model here proposed was not validated since it relies only on elements that are readily accessible in the TRNSYS libraries and have been previously authenticated [26]. In addition, the hydraulic analysis was carried out by using equations found in handbooks [27] or previously presented by Lickleder et al. [25].

2.1. Mass and energy balances

At each node of the network, it must be applied the mass conservation law and the first conservation of energy principle:

$$\sum_{i\in inlets} \dot{m}_i = \sum_{j\in outlets} \dot{m}_o \tag{1}$$

$$\sum_{i\in inlets} \dot{m}_i \cdot h_i = \sum_{j\in outlets} \dot{m}_o \cdot h_o \tag{2}$$

where $\dot{m}_i$ is the flow rate that enters the node and h_i is the specific enthalpy of the inlet flow rate. In addition, the subscript "o" refers to the outlet flows. In this case, it is assumed that the node is adiabatic and there is not any contribution of kinetic or gravimetric energy.

The energy balance for each user j is:

$$\dot{Q}_{user;j} = \dot{Q}_{pros;j} - \dot{Q}_{cons;j} - \dot{Q}_{stor;j} = \dot{m}_j \cdot c_W \cdot (T_s - T_r) \tag{3}$$

where $\dot{Q}_{pros;j}$ is the hourly production of heat (if user j is a prosumer), $\dot{Q}_{cons;j}$ is the hourly demand of heat (for DHW, Space Heating or Absorption chiller), $\dot{Q}_{stor;j}$ the power that is stored, c_w specific heat of the water, $\dot{m}_j$ mass flow rate through the user j, and T_s and T_r the supply and return temperatures respectively.

For the producers:

$$\dot{Q}_{pro;j} = \dot{m}_j \cdot c_w \cdot (T_r - T_s) \tag{4}$$

For storages in the district:

$$\dot{Q}_{sto;j} = \dot{m}_j \cdot c_w \cdot (T_s - T_r) \tag{5}$$

For the main power plant:

$$\dot{Q}_{gen} = \dot{m}_{\text{gen}} \cdot c_w \cdot (T_s - T_r) \tag{6}$$

where $\dot{m}_{\text{gen}}$ is the mass flow rate which flows through the main power plant.

The energy balance for the entire network is:

$$\dot{Q}_{gen} + \sum_{j=1}^{No.users} (\dot{Q}_{user;j}) - \sum_{j=1}^{No.producers} \left(\dot{Q}_{pro;j}\right) + \sum_{j=1}^{No.storages} \left(\dot{Q}_{sto;j}\right) + \dot{Q}_{losses} = 0 \tag{7}$$

where $\dot{Q}_{losses}$ are the environmental heat losses of the buried pipes calculated by using a TRNSYS component and its equations.

2.2. Pipes modelling

The selection of the DHN pipes is one of the most important step of a design of a DHN. In general, all the pipes used in a DHN are pre-insulated pipes [28] with a layer of insulation around a pipe made of steel or, more rarely, plastic. The research on the optimum between the minimization of pressure drops and the reduction of investment costs is still a hot topic in the scientific literature [29].

Once the flow rates in each branch of the network have been calculated from the mass and energy conservation, a hydraulic analysis must be carried out to determine the appropriate pipe diameters. This involves an iterative process of adjusting the diameters until the desired pressure drop in the most stressed branch is achieved.

The specific pressure drops $\Delta P_{s,i}$ in the branch i can be calculated using the Darcy–Weisbach relation [27]:

$$\Delta P_{s,i} = \frac{\Delta P_i}{L_i} = \frac{\lambda_i \cdot \rho_i \cdot v_i^2}{2 \cdot D_i} \tag{8}$$

In the previous equation, ΔP_i is the total pressure drop, L_i is the length of the pipe, λ_i the Darcy factor, ρ_i the density of the fluid and v_i and D_i are respectively the speed of the water and the diameter.

By using the Reynolds number Re_i on each branch i, and the roughness of the pipe ε_{pipe}, the Darcy factor is calculated as the same as [25] using approximations of the Colebrook-White relation:

$$\lambda_i = \begin{cases} \dfrac{64}{\mathrm{Re}_i}, \mathrm{Re}_i < 2000 \\ 4.36E(-6) \cdot \mathrm{Re}_i + 0.0233, 2000 \le \mathrm{Re}_i < 4000 \\ \dfrac{0.25}{\left[\log\left(\dfrac{\varepsilon_{pipe}}{3.7 \cdot D_i} + \dfrac{5.74}{Re_i^{0.9}}\right)\right]^2}, \mathrm{Re}_i \ge 4000 \end{cases} \tag{9}$$

No TRNSYS type can calculate the pressure trend in a network with not-smooth pipes, so basic hydraulic relations and equations (8) and (9) were implemented in a new component, Hydraulic Pipe – Type 496, created using the Fortran language. Utilizing inputs such as interior diameter, inlet pressure, and inlet flow rate, and parameters including density, viscosity, pipe roughness, and length, the model generates various outputs. These outputs include velocity, Reynolds number, Darcy Factor, pressure drop, and outlet pressure. The choice of using the diameter as an input permits the use of this pipe also for future optimization purposes. Specifically, the developed type initially calculates the fluid velocity based on the provided diameter, inlet mass flow rate, and fluid density [27]. Then, the Reynolds number is determined using parameters such as density, interior diameter, velocity, and viscosity [27]. Once the Reynolds number, roughness, and diameter are known, the Darcy factor is computed using Equation (9). Finally, the pressure drop in the branch is calculated as explained in Equation (8), and the outlet pressure is determined by simply subtracting the calculated pressure drop from the inlet pressure. By incorporating well-validated equations into a single type, the dynamic simulation of the hydraulic behaviour of DHNs on TRNSYS could be simplified.

To account for the thermal behaviour of the network, the proposed type is jointly solved with Type 31, already available in TRNSYS and named as “Pipe or Duct”. This type can calculate, given geometric data, inlet flow rate and temperature, and ground temperature, the heat losses and consequently the outlet temperature.

A preliminary study of thermal behaviour was conducted at first. This revealed that in the worst case, the difference in temperature between the first and the last user is below 6 °C, and this happens when the flow rate is at its minimum (on the night) leading to minimum pressure drops. In this situation, considering the difference between real values and the calculated mean temperature and pressures, an analysis carried out on EES revealed that the viscosity change is below 3% while for density this change is below 0.2%. For this reason, in the first version of this Type, the density and the viscosity are assumed constant.

2.3. Main power plant and heating loads

The centralized power plant should satisfy the needs of each building in the cluster [30]. It must produce heat at the highest temperature required by the buildings’ heating systems, so the correct production system must be carefully chosen (gas turbine, alternative engine, solar collectors’ plant, etc.). Since the main interest of this paper is to focus on the DHN, the CHP unit and the loads are modelled just through basic equations and datasheets. The CHP will provide hourly thermal energy to satisfy all the needs (applying equation (7), and its flow rate strictly depends on loads.

It is necessary to choose the type of connection between the network and the users. In the case of prosumers, the grid connection requires a specific connection and substation scheme study. For instance, it can be return-supply if the temperature of the source is hot enough or, vice-versa it can be a return-return configuration in which the water is taken from the return pipe and fed back into the return pipe after being heated. Lennermo et al. [31] suggested a good substation configuration to achieve proper flow and pressure.

To simulate the DHN of the case study, the flow rate needed by each user is first calculated for each timestep by fixing the variation of temperature between the supply and return ring and by knowing the thermal demand of the building. Controlled flow diverter valves and tee pieces TRNSYS types are used to manage the flow rates between hot and cold rings.

In the case of consumers, the tee piece is connected with the return loop and the diverter valve with the supply one while in the prosumer substations, there are also diverter valves in the supply side and tee pieces in the return one.

Since the valve need as input a control value (where 1 means that all the flow is directed to the user and 0 to the next branch), an algorithm has been developed:

$$Control = GT\left(\dot{Q}_{cons}, 0\right) \cdot \frac{\dot{m}_j}{\dot{m}_{in}} = 0 \tag{10}$$

where $\dot{m}_{in}$ is the flow rate coming from the previous branch. In this equation if there is a consumption of heat from the user j, the flow rate $\dot{m}_j$ will be drawn from the hot side. For prosumers the same algorithm is applied, using $\dot{Q}_{prod}$ in case of heat production and water injection on the supply side.

2.4. CO_2 emissions estimation

As previously mentioned, 4th generation DHNs are more sustainable due to the use of RES such as solar collectors or PV panels for power-to-heat technology. According to this, the following equation is used to calculate the hourly emissions m_{CO_2} associated with the operation of the DHN:

$$m_{CO_2} = W_{pump} \cdot f_{el} + \frac{Q_{gen}}{\eta_{CHP} \cdot LHV_{NG}} \cdot f_{NG} \tag{11}$$

where W_{pump} is the energy consumption of the pumps, LHV_{NG} the lower heat value of the Natural Gas used by the CHP, f_{el} and f_{NG} are respectively the conversion factor for CO_2 of the electricity and the natural gas. The efficiency η_{CHP} of the generation system depends on the load factor and the dry bulb temperature of the air. According to the method used in [29], utilizing data derived from an accessible gas turbine [15], an efficiency curve was modelled assuming air temperature and load factor as the most influencing variables. This allows for the computation of

hourly natural gas consumption.

3. Description of case study and scenarios

During the operation of a DHN, since the heat demanded by buildings changes continuously, the flow rates in the DHN change too. This means that also the pressure along the network changes as well. The TRNSYS model developed in this study aims to evaluate the main thermohydraulic properties of the grid on an hourly basis. The main parameters considered are pressures, flow rate, temperatures, and energies.

TRNSYS is a software that allows transient systems to be simulated and it is mainly used for studies of energy and electrical systems, and it is also used for DHC systems. The software consists of two parts: the first is the system of algorithms that processes the input file, studies, and verifies the convergence of the equations system, solves it, and provides the required output. The second part is an extensive library of energy and electrical components (called Types) available for the composition of the system, and it is also possible, using a calculator type, to insert different equations (made up of input and output) that can compensate for the lacks.

3.1. Case study

For the case study, a cluster of 10 users has been considered. The cluster is in Palermo, in the South of Italy where cooling loads prevail over the heating ones. In particular, Palermo belongs to the B climatic zone according to Italian legislation [32] and it is characterized by 751 heating degree days. In Fig. 1 there is a representation of the network and its users. In particular, in a clockwise direction: power plant, hotel, six small 3-storey apartments, first office, secondary school, second office, four big 3-storey apartments, 20 small houses, hospital, primary school and 3 10-storey apartments.

It is clear from Fig. 2 that in Palermo, building cooling loads are greater than building heating loads. This is primarily because of the local climate, where the outside air temperature rarely drops below 10 °C. Contrarily, when solar radiation is more intense in the summer, there is a corresponding temperature rise, which necessitates a greater cooling load in order to maintain a comfortable environment within the buildings.

The demands of hotels, offices, and the hospital have been previously estimated in another research work [33], where ad hoc energy audits have been performed by the authors. Regarding other groups of buildings, demand profiles were obtained from the simulation performed on Energy Plus [34], using the archetypes of buildings available in [35], considering the buildings for a warm-humid climate, which represent the climate zone of Palermo [36], and considering climate data available in [37]. Each user is indirectly connected to the DHN via a substation. The power plant will generate heat in all seasons, it directly feeds the exchangers in heating mode, and it supplies the absorption chillers which are installed in each user in summer.

In this case study, the maximum contemporaneous demand of heat is 9.44 MW on July 18th during the cooling season for feeding the absorption chillers as can be seen in Fig. 3. It is chosen to consider a central plant made of two gas turbines. More specifically, the first one with an electrical nominal capacity equal to 3 MW and the second one 500 kW. Thanks to this configuration, it is possible to partialize the thermal capacity from 10 MW to below 100 kW, so all the loads can be covered. To simulate the gas turbine CHP, efficiency curves available in [29] have been utilized to calculate the required fuel for generating the desired heat.

Table 1 provides details on the thermal requirements of each user of the district. Despite its small size, the district interacts with a diverse range of end-users, cumulatively necessitating a concurrent thermal demand of 9.4 MW. Certain facilities, such as offices and schools, exhibit a low load factor due to reduced demand during nighttime hours. Conversely, residential buildings and hotels demonstrate a higher load factor, reaching up to 36%, reflecting their consistent thermal needs.

Cooling energy is supplied by absorption chillers installed at each user. In this way, the buildings just need heat from the network to supply both heating and cooling. The chiller chosen has a COP of 0.7 which was assumed to be constant.

The flow rate of each user is controlled by a two-way control valve. In the case of prosumers, the connection with the grid requires, to supply water from the return to the supply side, local variable speed pumps following the scheme suggested by Lickleder et al. [25]. The distances

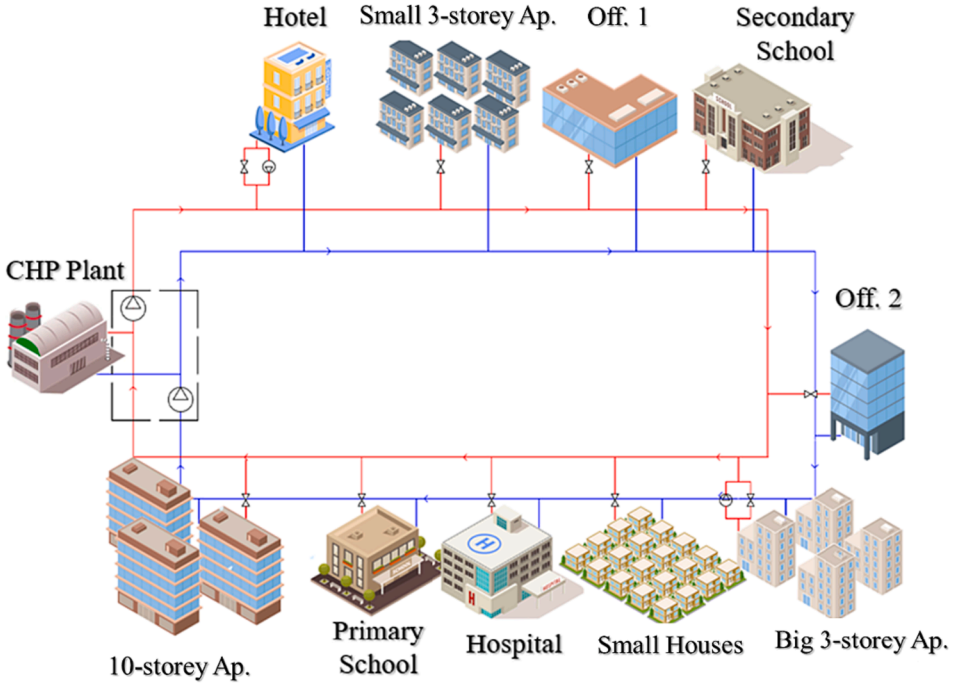

Fig. 1. Case study network.

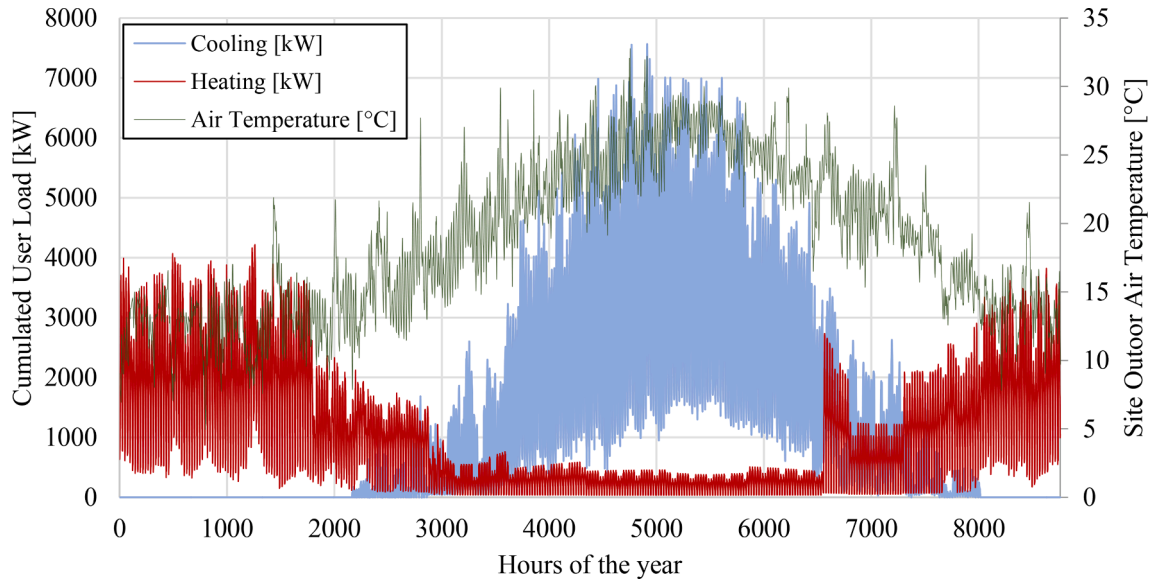

Fig. 2. Cumulative user loads and outdoor air temperature in the case study.

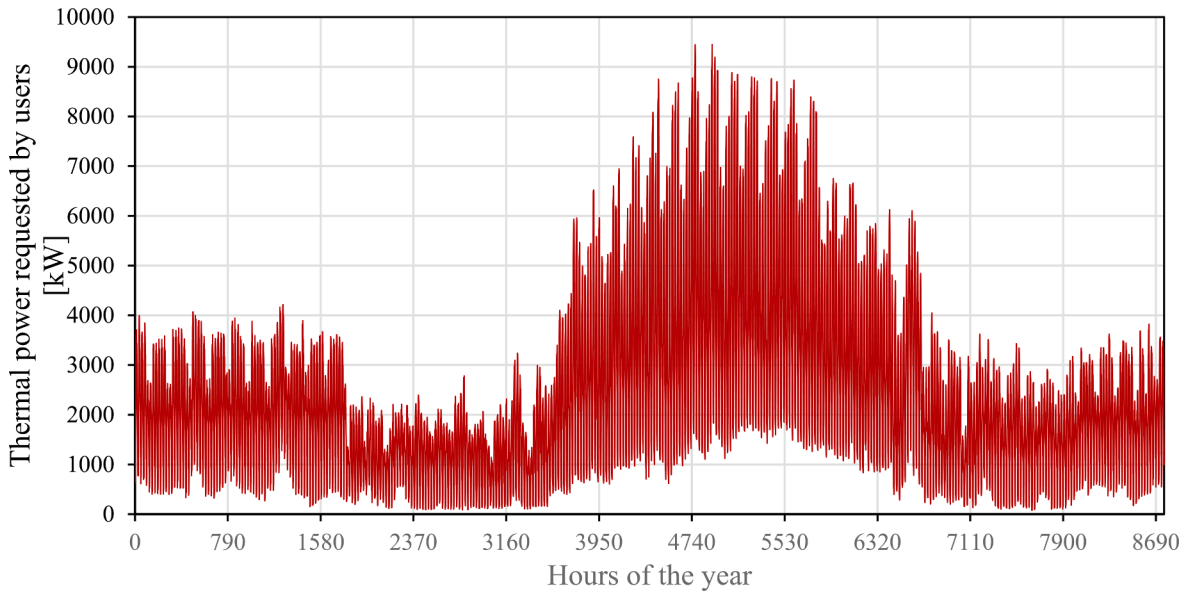

Fig. 3. Overall thermal load for all the buildings in the case study.

between each user are fixed at 200 m to avoid any divergence in the results that could depend on the distances.

All the equations mentioned before can be solved by imposing a value for the speed or the diameter. In this case, it has been proceeded iteratively using the commercial diameters found in a technical brochure. Both loops have been designed with the same single diameter to avoid section reduction and because the location of maximum flow rates could change because of the presence of prosumers.

3.2. Network design on TRNSYS

The following types were included in the dynamic modeling to simulate the operation of the DHN:

- Type 11f: Controlled flow diverter. This is used to divert the flow rate from the supply ring to the return one (the opposite for the producers). This is controlled by the equations on the substation and simulates a 2-way valve installed at each user.
- Type 11 h: Tee-piece. This is used to mix the flow rate from each substation to the one in the cold ring.
- Type 31: Pipe/Duct. It is used to simulate the heat losses with the ground.
- Type 496: Hydraulic Pipe. Type developed in this work for hydraulic calculations.

Using these types in addition to other data readers and equations, it is possible to determine the hourly time series of flow rates and temperatures in the network. Fig. 4 represents the DHN model developed in TRNSYS. To quantify the heat losses in the pipes, the loss coefficient has been calculated using the data from the brochure previously noted and the ground temperature has been set as the environment temperature.

The initial pressure on the supply side is imposed at 9 bar, while on the return side, it is set at 7 bar. These values were selected to facilitate the visualization of pressure drops in each branch under various operating scenarios.

The primary focus of the modeling was investigating the thermal

Table 1
User and cumulative thermal load.

	Total Thermal Energy	Maximum Thermal Power	Mean Thermal Power	Load Factor
	[MWh]	[MW]	[MW]	[-]
Hotel	6839.78	2.19	0.78	36%
Small 3-storey apartments	1664.80	0.62	0.19	30%
Office 1	1215.69	1.18	0.14	12%
Secondary school	1456.61	1.07	0.17	16%
Office 2	868.35	0.84	0.10	12%
Big 3-storey apartments	1494.51	0.78	0.17	22%
Small houses	773.54	0.42	0.09	21%
Hospital	3477.77	2.05	0.40	19%
Primary school	798.60	0.43	0.09	21%
10-storey apartments	2727.34	1.48	0.31	21%
Total	21316.99	9.45	2.43	26%

behaviour of the DHN. TRNSYS types including Type 31 "Pipe or Duct," Type 11f "Controlled flow diverter," and Type 11 h "Tee piece" were initially used for the creation of the dual-loop model. The calculation of the thermal side's behaviour during the year-long simulation in terms of flow rates, temperatures, and energy balances was made possible by the integration of these three types, together with calculators for controls, datasheets, and weather files. The thermal model is inextricably tied to the hydraulic computation because Type 496 uses the flow rates from Type 31 as inputs. Finally, this type provides a dynamic stationary analysis of the pressure drops in each branch and the pressure at all nodes based on the equations previously described in section 2.2.

3.3. Description of the investigated scenarios

Different scenarios were assumed to study the variations of thermohydraulic parameters of the DHN under different operating conditions. Differences in energy savings and emissions between all the scenarios will be discussed.

Base Case. It represents a 3rd generation network in which all users are consumers. The design temperatures are 100 °C on the hot side. The high temperatures are chosen to be compatible with a 3rd generation DHN but also with the production of cooling energy through absorption chillers installed at each user. A plant, made by three CHPs operating in parallel, generates the heat needed by all the users.

Scenario 1. In the first scenario, the potential of 4th generation DHNs is investigated. During the autumn, winter, and spring months, the supply side of the grid operates at temperatures of either 80 °C or 60 °C to minimize heat loss, so called respectively scenario 1a and 1b. However, during the cooling period, the grid must operate at 80 °C due to constraints with the operation of absorption chillers. In this scenario, a field of evacuated tube solar collectors with a total power output of 7 MW_p in order to increase the share of RES in the grid. This scenario aims to demonstrate the advantages of lowering the temperature of a DHN such as reduction in thermal losses and integrating solar collectors into the system.

Scenario 2. In this scenario, the supply temperature is 60 °C in the

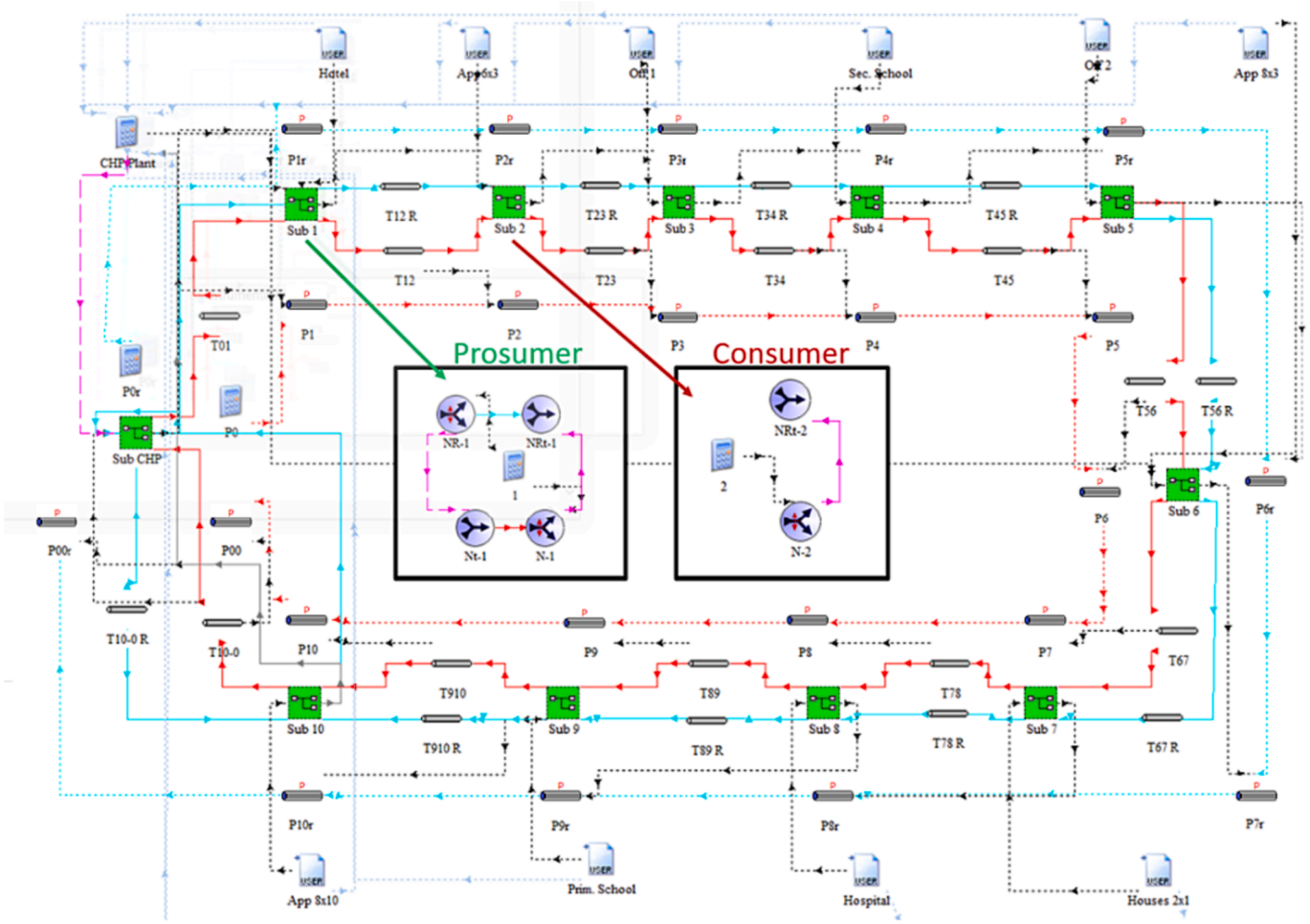

Fig. 4. Case study DHN model developed on TRNSYS.

heating period and, to support the solar field and the CHP, two consumers become prosumers in the period between December 1st and 31 March 31st. In the context of high-RES penetration, these users will be producers during the solar peak hours (11 am to 2 pm). Each of them has an HP, with a capacity of their maximum load, that they use for self-consumption and during peak solar hours the HPs work at full load, feeding the surplus of heating energy into the grid. This scenario will show the difference in terms of pressure when a prosumer helps the CHP and there will be energy savings.

4. Results and discussions

All scenarios have been simulated and the results are presented in this section. For each, the analysis will focus on pressure, temperature, energy savings, and emission reduction.

4.1. Results for the Base case

A preliminary analysis in steady-state operation was carried out for designing the DHN. The Euroheat Guidelines [38] recommend operating pressures of 6 bar for districts operating at 90 °C and 16 bar for districts operating at 110 °C. For this reason, modern districts are kept between 6 and 10 bar. The choice of the diameter of the pipes is linked to the specific pressure drops in every branch of the network [39], for instance, the Swiss guide for the DHC system suggests specific pressure drops between 150 and 250 Pa/m [40].

The most stressed branch, in this case, is the one in the supply loop after the main production plant and, considering the maximum loads of each user, the iteration results suggested to select the following diameter value for the DHN:

- $D_{01} = DN250(263,7mmD_i)$
- $\Delta P_{m;01} = 140.2 \frac{Pa}{m}$

In order to avoid an anomalous increase in pressure drops when a prosumer injects heat into the network, the same diameter for each pipe in the network has been considered. Since the same length of 200 m has been chosen for each pipe, the total length of one ring of the district considered measures 2.2 km.

In the case study considered, as can be seen in Fig. 5, the typical trend of pressures in a double loop DHN is achieved [20], guaranteeing a differential pressure of 1 bar at the most stressed user.

At first, the network has been simulated under standard conditions. A comparison will be made, as possible, to the other cases. In this scenario, it was assumed that the presence of no other producer than the power plant, and the temperature of the supply ring is the highest possible (100 °C).

As illustrated in Fig. 6, the pressures just before the pumps, represented by P_0* and P_0* R, are lower during the summer than during the winter. This is due to the higher flow rates during the summer months when the cooling load exceeds the heating load. During winter, the maximum pressure drop, measured before and after the pump, is 0.13 bar for the supply side and 0.26 bar for the return side. During the cooling period, it is 0.91 bar in the hot ring and 0.85 bar in the cold ring.

The difference in pressure drops between the two rings is more pronounced in winter. This is because users at the end of the network, primarily residential buildings, do not require as much heating energy. As a result, less water flows through the last part of the supply side compared to the return side, where flow rates reach high values in branches near the CHP system.

As shown in Table 2, the total electric energy requested for pumping in winter is 2.06 MWh and it is 21.5% of the summer. It is also interesting to notice that during winter the supply pumps need 49.3% of electricity than the other side.

Focusing on the pressure profiles in Fig. 7 it is possible to notice that the pressure drops are almost negligible at night due to the lower heat demand (mainly by the hotel and the hospital). During winter, this situation leads to a reduction in total demand whose average value is 141.8 kW for nights and 501.2 kW for the rest of the day. The DHN is designed to operate in the worst condition when the load reaches its maximum. For this reason, when the flow rate decreases the pressure values are almost equal to the nominal value. In summer this difference is more emphasized since in the nighttime, the mean flow rate processed by the CHP is just 23.7% of the mean flow rate during the daytime.

Table 3 shows the changes in pressure decreases for two representative hours on a typical winter and summer weekday for each branch of the district. The table shows that on the supply side, the first branch is the most stressed while, on the return side, this happens for the last one. It is important to notice that through the last branch of the supply side and the first branch of the return side, the pressure drops are practically negligible, as only a minimal flow rate passes through these branches. These results also highlight the fact that the total pressure drops during summer are almost 32 times larger for the supply side and 10 times higher for the return than those during winter.

Temperatures in each node of the grids vary mostly with the flow rate. For instance, at night, when the flow rates are low, these begin to drop, while during the day the drops are lower (Fig. 8). During the year the heat losses are stable and, since they depend on temperature, the losses on the supply calculated are 582.4 MWh and these are higher than the return side of factor 1.3.

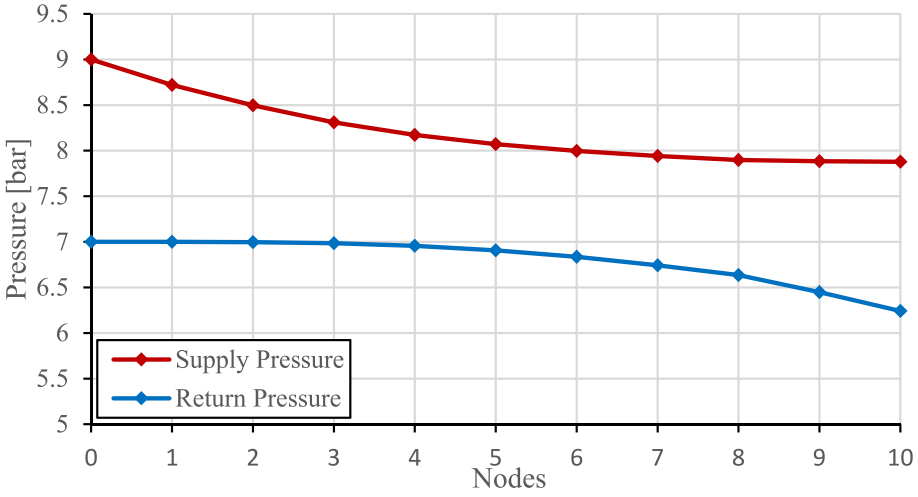

Fig. 5. Trend of pressure for each node of the network in the design phase.

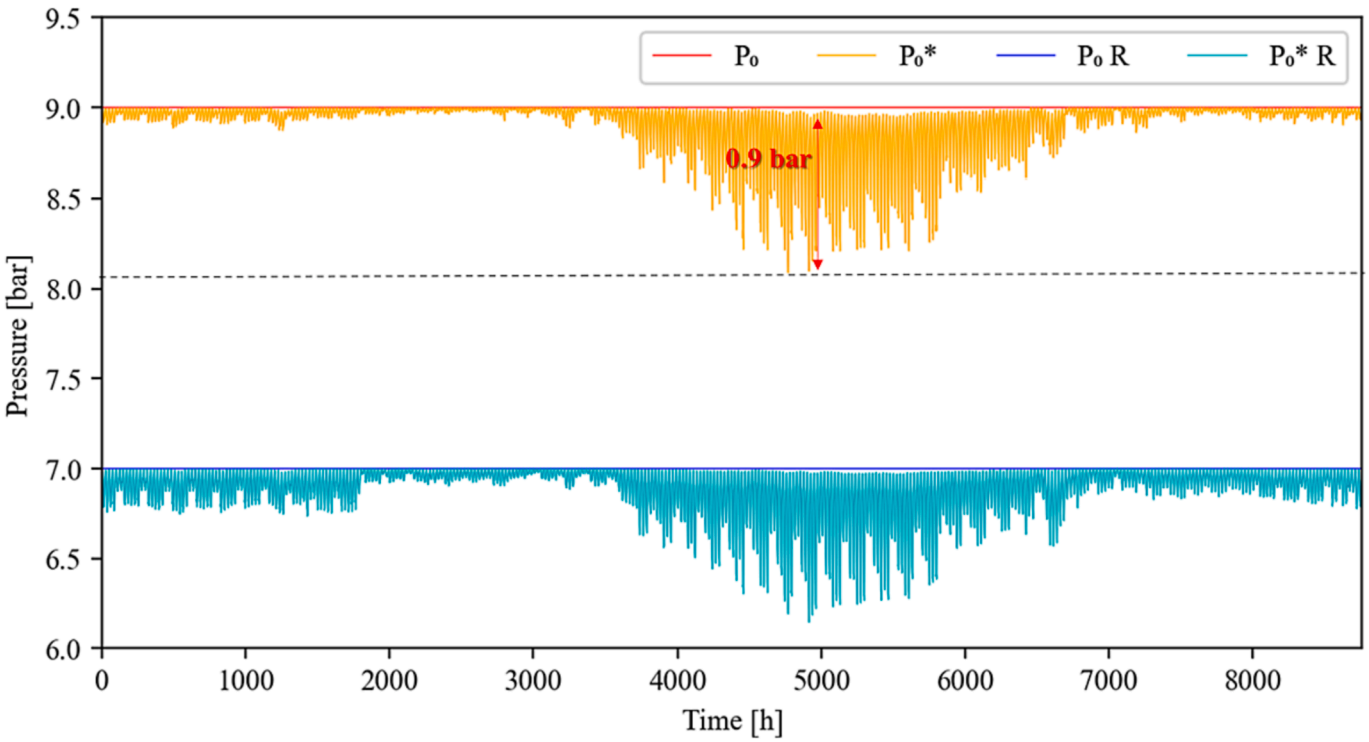

Fig. 6. Hourly pressures, on the sides of the pump, during a year in the DHN.

Table 2
Electric Energy requested by the pumps.

	Winter Energy	Total Energy	Max power in winter	Max power during the year
	[MWh/y]	[MWh/y]	[MW]	[MW]
Supply pumps	0.681	5.772	0.002	0.012
Return pumps	1.384	5.88	0.003	0.010

The variation of temperature between the first and last node is higher in winter than in summer. As previously explained, it is a consequence, of the lower flow rates in winter (especially in the last branches). In this situation, despite the higher variation of temperature in a branch, the losses are not the highest, because they depend strictly on the flow rates.

To ensure thoroughness, a comparative analysis of temperatures and pressures during standard hours was performed between the TRNSYS and stationary models developed on EES [41].

As illustrated in Fig. 9 and Fig. 10, differences in the results from the dynamic and stationary models are minimal. The maximum relative error for pressures is 0.7%, while for temperatures it is 2.1%. In addition, it should be noted that the greatest error in pressure behaviour occurs during periods of high demand (e.g., summer), whereas the maximum temperature error occurs when the load is very low (e.g., spring). This can be attributed to the fact that as the load increases, the flow rate and pressure drop increase, while the temperature variation in each node decreases (as depicted in Fig. 10). In both cases, the error becomes higher with distance from the CHP, making it more noticeable in larger DHNs.

4.2. Results for Scenario 1

Scenario 1 is characterized by the transition to lower temperatures. The network starts operating at 80 °C and then at 60 °C. In this way, it is possible to feed the users only for heating, because at 60 °C the grid cannot feed the absorption chillers installed in each user. The network will be managed with a supply temperature of 80 °C only in the conventional cooling period in Palermo, from June 1st to September 30th. Lowering the operating temperature of the grid, it is easier for the prosumers to assist the power plant, a hypothesis that has been analysed in the third scenario.

The variation of temperature during the day will decrease too when lowering the temperature (Fig. 11), indeed, the mean variation for all the heating period decreases from 7.26 °C to 3.83 °C in the case of 60 °C.

In Table 4 it is possible to notice that a lower temperature leads to considerable energy savings. In this case study, considering only at the heating period, the heat losses are reduced, compared to the Base Case, by a factor of 1.36 in the case of a DHN temperature equal to80 °C. and by 2.12 for a DHN temperature equal to 60 °C. The yearly energy losses variates between 1040 MWh (Base Case) and 475 MWh (Scenario 1b) corresponding to only 4.9–2.2% of the total heating energy requested by the users (Table 1).

In Scenario 1, thanks to the reduction of supply temperature, the main central plant is also supported by a 7 MW_p solar field composed of evacuated tube collectors connected with the district by a 5 m^3 storage/heat exchanger. The flow rate drawn from the return ring is pre-heated in the exchanger and if the temperature is below the setpoint the water reaches the CHP which produces the necessary heat for reaching the desired temperature. In scenario 1b, it is possible to save 5564 MWh of heating energy which is produced by the solar collector reducing the total energy produced by the CHP by 25.5%. It is interesting also noticing that, while in full demand periods (such as summer or winter) the solar collectors only pre-heat the water. In low-demand periods (such as spring or autumn) during the solar peak hours the DHN is fully fed by the solar field leading to the previously cited energy savings.

4.3. Results for Scenario 2

As already mentioned, in this scenario, the hotel and the big 3-storey apartments become prosumers as well. The logic of energy production is simple: the electric network operator asks these users to use their HPs at

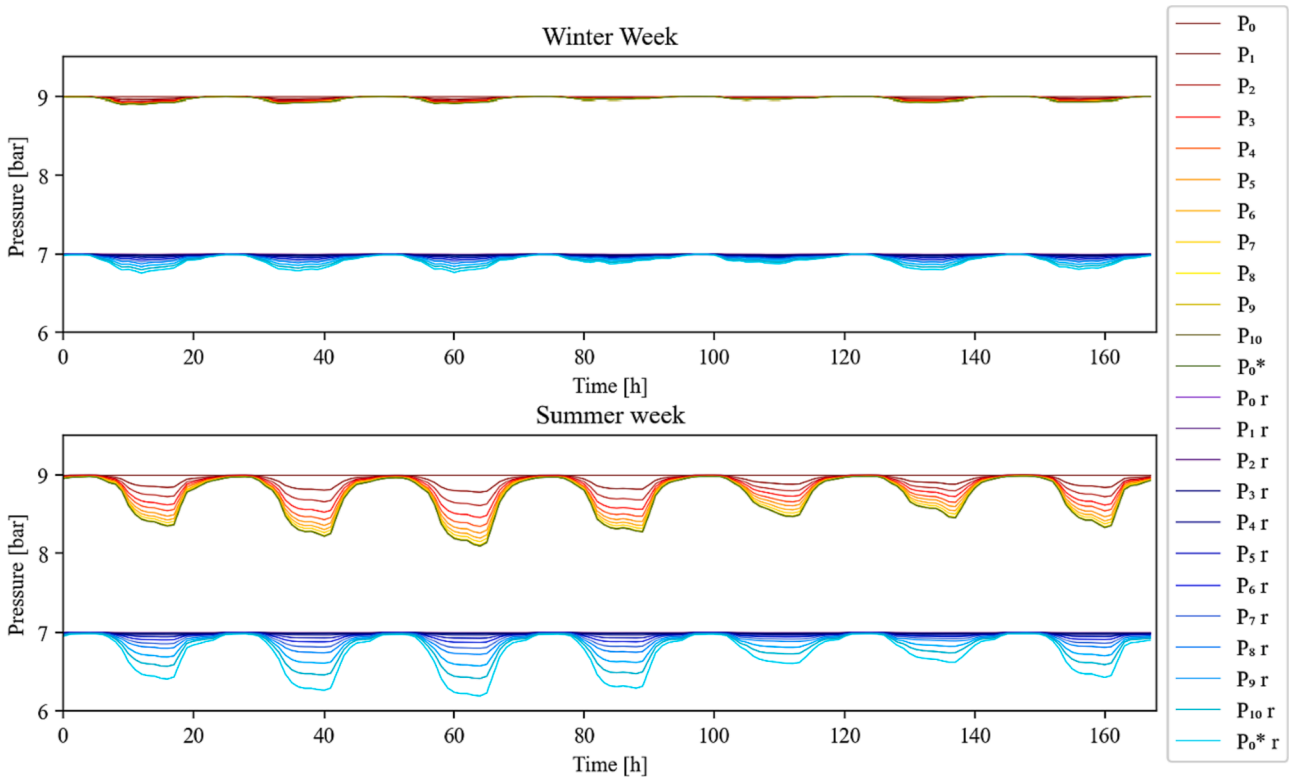

Fig. 7. Hourly pressures during standard weeks in the DHN.

Table 3
Pressure drops in network branches.

		Total	0–1	1–2	2–3	3–4	4–5	5–6	6–7	7–8	8–9	9–10	10–0*
		[kPa]	[kPa]	[kPa]	[kPa]	[kPa]	[kPa]	[kPa]	[kPa]	[kPa]	[kPa]	[kPa]	[kPa]
Supply Side	Wint. Week	2.59	1.28	0.31	0.17	0.17	0.17	0.17	0.15	0.13	0.01	0.01	0.00
Return Side		7.86	0.00	0.40	0.58	0.58	0.58	0.58	0.62	0.65	1.09	1.09	1.72
Supply Side	Sum. Week	82.82	20.99	15.53	14.32	10.21	7.44	5.30	4.15	3.74	0.74	0.39	0.00
Return Side		78.05	0.00	0.57	0.84	2.30	3.93	5.77	7.07	7.61	14.21	15.87	19.89

full load, from 11:00 AM to 2:00 PM, to absorb the electricity surplus due to a high-RES penetration. Specifically, the system incorporates a high-temperature air-to-water HP which uses the outside air as the source. This HP draws water from the return side, heats it to the predetermined setpoint temperature, and subsequently injects the heated water into the supply side. In this case, the supply temperature must be settled at 60 °C, so their contribution can not be evaluated in the cooling period (from the 1st of June to the 30th of September in Palermo). During these three hours, they will generate hot water when the capacity of the HP, designed on the maximum heating load, is higher than their load. In summer they just do not receive heat from the network, so their loads are set to zero in those hours.

When the generation is distributed the pressure level will change among the network. The pressure drops decrease when the prosumers inject because the flow rate gets distributed more regularly (Winter Week in Fig. 12), but it also decreases when the two consumers do not request heat, as in the summer case (Summer Week in Fig. 12). These differences emerge by comparing Fig. 12 with Fig. 7.

During the winter months, the energy required for pumping is 73% of that required in the Base Case for the same period. For the remainder of the year, assuming that two users do not require heat in the grid for 3 h per day, the energy savings amount to 1.5 MWh, or 15.5% of the Base Case energy. When comparing the results of Scenario 2 with those of Scenario 1, it can be seen that the heat production avoided by the main plant due to the presence of prosumers amounts to 1265 MWh which represents 7.8% of the total for Scenario 1 and 31.3% for the Base Case. Focusing solely on the heating period when prosumers are active and the network operates at 60 °C, the energy savings compared to Scenario 1 reach 11%.

It is crucial to keep in mind that the situation under consideration is influenced by the location and size of the prosumer, as well as the length of the connections. Therefore, in the proposed methodology, the prosumers are positioned at two distinct points within the network, while keeping the pipe length and diameters constant.

4.4. Discussion on energy savings and environmental impact

Table 5 summarizes the improvements observed in each scenario. Only the results of scenario 1b are included in the table, since the difference in energy losses between scenario 1a and 1b is negligible, being about 2% of the energy generated by the CHP. As expected, Scenario 2 is the optimal scenario in terms of energy savings, as the CHP needs to produce 31.3% less thermal energy than the base case. The comparison between Scenario 1b and Scenario 2 shows that both have similar heat losses since the operative temperature is the same, but prosumers interaction in Scenario 2 enables saving 1266 MWh of thermal energy. The electric energy required for pumping is the same between scenario 1b and Base Case since no prosumers are considered and the network is

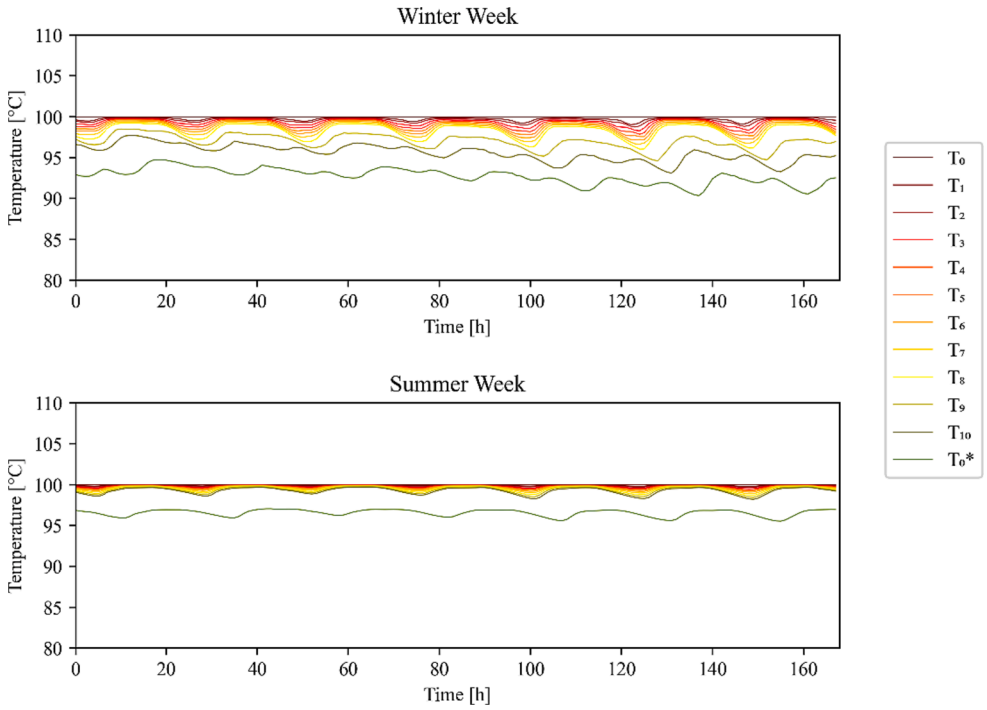

Fig. 8. Hourly temperatures during standard weeks in the DHN.

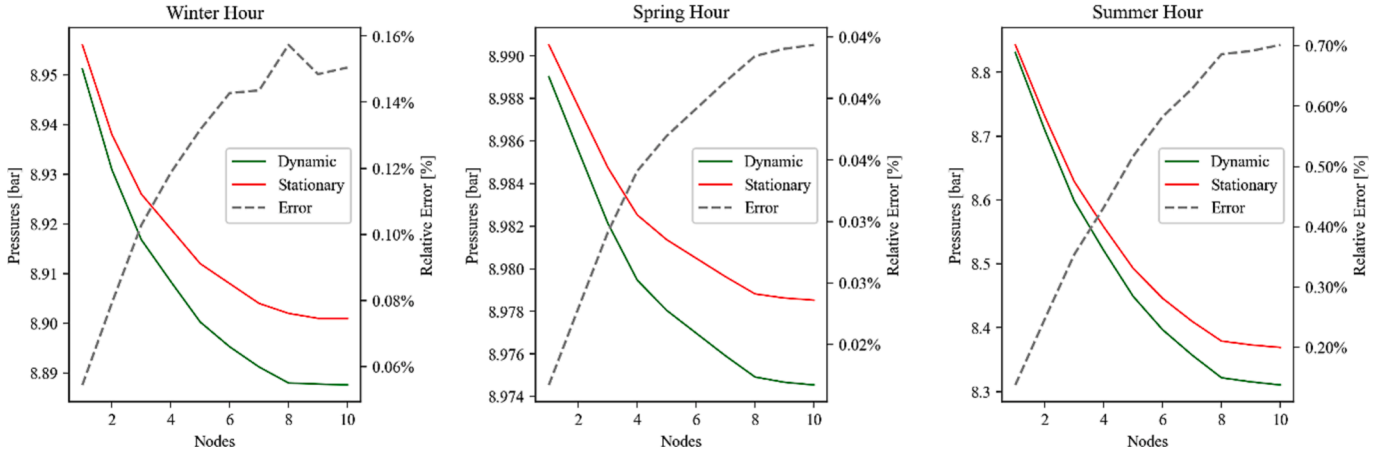

Fig. 9. Pressures comparison during standard hours.

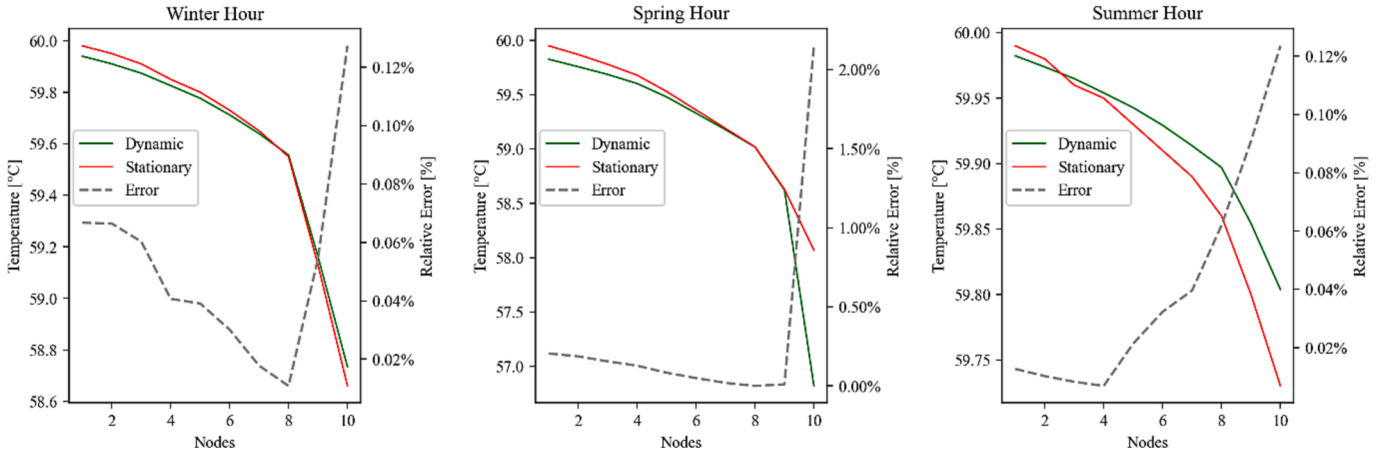

Fig. 10. Temperatures comparison during standard hours.

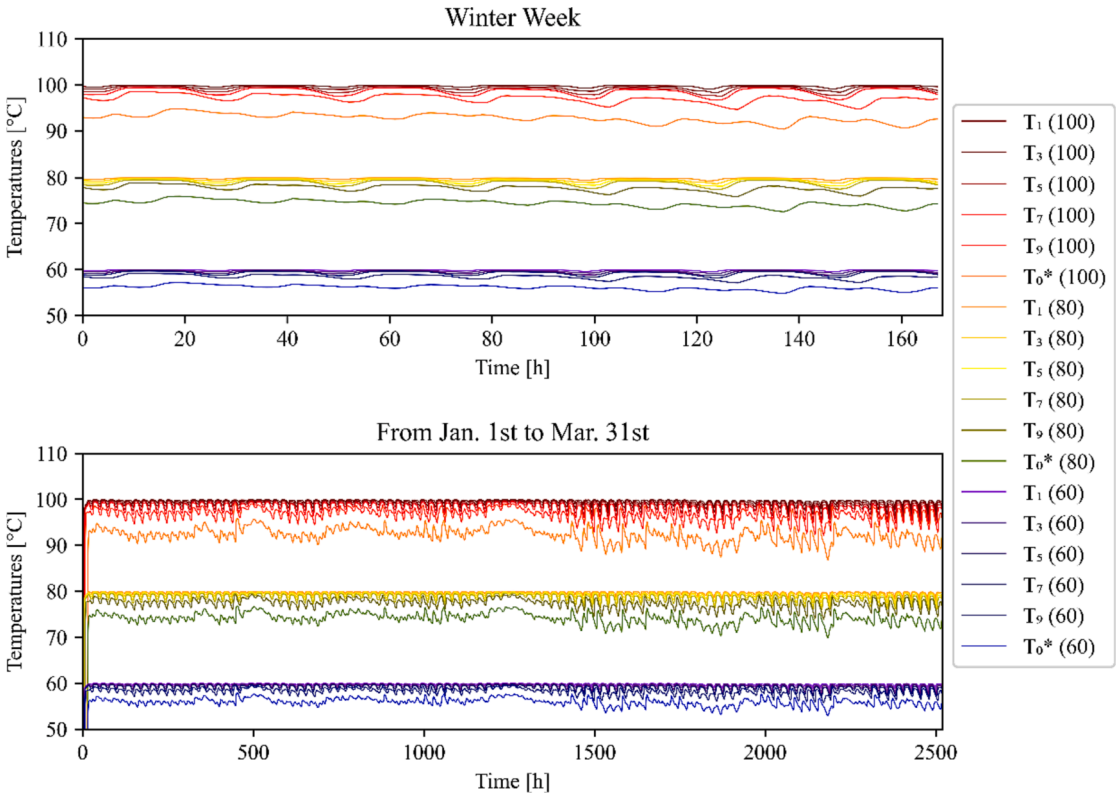

Fig. 11. Hourly temperatures of some supply nodes in a DHN operating at 3 different temperatures (100 °C, 80 °C, 60 °C).

Table 4
Heat losses in the pipes during winter.

	Supply Heat Losses	Return Heat Losses	Mean ΔT	Maximum ΔT
	[MWh]	[MWh]	[°C]	[°C]
Base Case (100 °C)	395.21	313.64	7.24	13.80
Scenario 1a (80 °C)	302.02	219.50	5.53	10.60
Scenario 1b (60 °C)	208.83	125.34	3.83	7.40

managed in the same way. As discussed in the last section, the injection of prosumers leads to an overall energy saving of 2 MWh.

In terms of the energy efficiency, Scenario 2 outperforms the others. To quantify CO_2 emissions, both the electricity consumed by the pumps and the fuel consumption of the CHP must be considered (Table 6).

The avoided impact of CO_2 can be calculated using the emission factor for the production of electricity in Italy which amounts to 307.7 gCO_2/kWh [42]. Thanks to the benefits in terms of a more regular pressure level, in Scenario 2 the energy savings for pumping operation amounts to 2.05 MWh which corresponds to an avoided production of CO_2 of 0.63 t, which is 17.6% less than the Base Case.

In Scenario 2 the fuel consumption of the CHP is the lowest. This happens for two reasons: first the network operates at a lower temperature, 60 °C instead of 100 °C, and this reduces the heat losses. Second, two users, who became prosumers, supply heat to the DHN in winter and reduce the heat demanded to the CHP.

To quantify the emission reduction due to the lower NG consumed by the CHP plant, an emission factor of 227.31 gCO_2 for 1 kWh of natural gas was considered according to [43]. The findings indicated a reduction in CO_2 emissions by 2803 t, which constitutes 31.3% of the emissions in the Base Case scenario.

5. Conclusions

It is widely known that DHN evolution plays a key role in decarbonization of the energy consumption in cities. Previsions show that this technology will spread around the world, especially in developing countries, so it is essential to propose solutions efficient and environmentally and economically sustainable. Future DHNs must be managed in such a way that they allow the integration of heat produced from renewable sources to contribute to reducing emissions. As illustrated in this paper, this requires lowering the temperature of the district and new management ideas must be proposed to allow the use of renewable sources.

The analytical model developed in this paper can be used to perform analysis in dynamic but also in steady-state (to design the DHN), considering the presence of prosumers. After a few mentions of the analytical model, the case study is presented to investigate the thermohydraulic variables of the system during operation. Some necessary components and other equations, for pressure analysis, were chosen to model the DHN in TRNSYS. Three different scenarios have been modelled The Base Case refers to a classic 3rd generation DHN without prosumers and this case has been compared to two scenarios of gradual improvement. In Scenario 1 the supply temperature of the network has been lowered from 100 °C to 80 °C and then to 60 °C and a field of evacuated tube solar collectors was integrated with CHP. Considering only the heating period, lower operating temperatures led to 26.4% and 52.8% of reduction in thermal losses, respectively for the 80 °C and the 60 °C supply temperature. Moreover, the inclusion of solar collectors led to heating energy savings above 25%. In the last scenario, the supply temperature was set at 60 °C for the heating period and two prosumers were assumed. Specifically, the prosumers produced heat by HPs. Focusing on the heating period, the results showed that this solution led to energy savings of 27% for pumping and 31.3% reduction of the thermal energy requested to CHP. CO_2 emissions of the system were quantified, and results showed that the total emissions related to

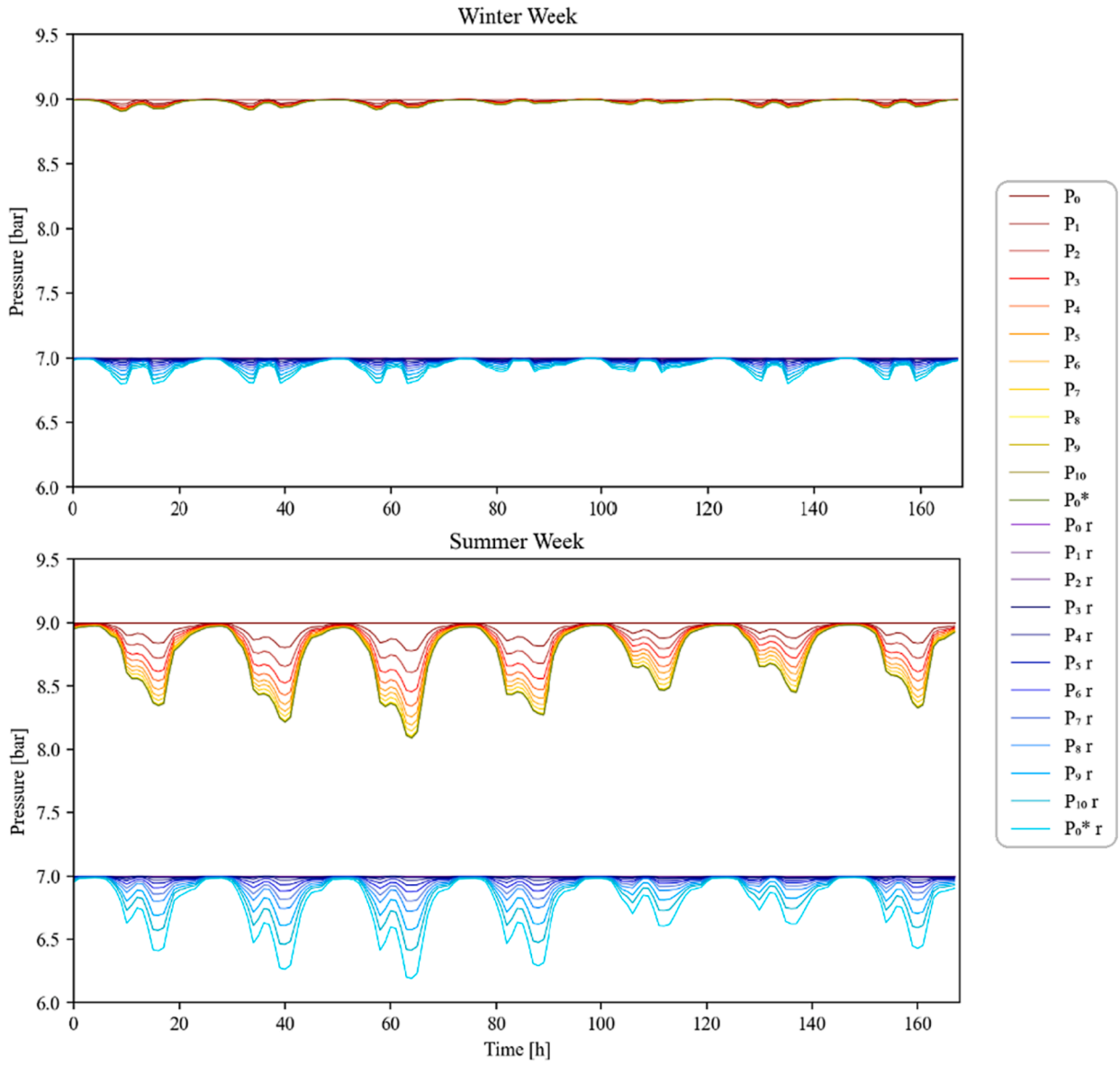

Fig. 12. Pressures distribution on a winter and on a summer week in Scenario 2.

Table 5
Main results for each scenario.

	Energy generated by CHP	Energy generated by RES	Heat Losses	Energy for Pumping
	[MWh]	[MWh]	[MWh]	[MWh]
Base Case	21,793	0	1040	12
Scenario 1b	16,229 **(-25.5%)**	6040	475	12
Scenario 2	14,963 **(-31.3%)**	7305	475	10

Table 6
CO_2 emissions in the main cases of the case study.

Cases		CO_2 for pumping	CO_2 for heat production	CO_2 hourly emissions
		[t/y]	[t/y]	[kg/hr]
Base Case	Winter	0.64	4526.34	0.78
	Total	3.59	8952.96	1.02
Scenario 2	Winter	0.46	3101.12	0.53
	Total	2.95	6149.44	0.70

Scenario 2 are only 68.6% of the Base Case. The model was proved to successfully work under different conditions. Indeed, the hourly results showed the capability to monitor the thermohydraulic behaviour of the DHN, and it could assist to develop innovative management solutions. The same model can be applied to various scenarios because it just needs inputs such as climate data, pipe data, and load description. Further analysis will comprehend more realistic prosumers and implementation of a substation for detailed flow rates and studies on district cooling. The same model, through appropriate changes in the equations, could be also adopted to simulate a 5th generation DHN.

CRediT authorship contribution statement

T. Testasecca: Conceptualization, Methodology, Software, Investigation, Writing – original draft, Visualization. **P. Catrini:** . **M. Beccali:** Conceptualization, Methodology, Investigation, Writing – original draft, Writing – review & editing. **A. Piacentino:** Conceptualization, Methodology, Investigation, Resources, Writing – review & editing,

Supervision.

Declaration of Competing Interest

The authors declare that they have no known competing financial interests or personal relationships that could have appeared to influence the work reported in this paper.

Data availability

No data was used for the research described in the article.

References

[1] European Commission, "Building and renovating: The European Green Deal," no. December, pp. 1–10, 2019, doi: 10.2775/48978.
[2] IEA, "Heating." [Online]. Available: https://www.iea.org/reports/heating.
[3] IEA, "How can district heating help decarbonise the heat sector by 2024?" [Online]. Available: https://www.iea.org/articles/how-can-district-heating-help-decarbonise-the-heat-sector-by-2024.
[4] Gestore dei Servizi Energetici, "Teleriscaldamento e Teleraffrescamento 2019. Nota di approfondimento GSE," 2020.
[5] Weiss W, Spörk-Dür M. "solar Heat Worldwide" 2022.
[6] Lund H, et al. Perspectives on fourth and fifth generation district heating. Energy 2021;227:120520. https://doi.org/10.1016/j.energy.2021.120520.
[7] Werner S. International review of district heating and cooling. Energy 2017;137:617–31. https://doi.org/10.1016/j.energy.2017.04.045.
[8] Sorknæs P, et al. The benefits of 4th generation district heating in a 100% renewable energy system. Energy Dec. 2020;213. https://doi.org/10.1016/j.energy.2020.119030.
[9] O. Todorov, K. Alanne, M. Virtanen, and R. Kosonen, "Aquifer thermal energy storage (ATES) for district heating and cooling: A novel modeling approach applied in a case study of a Finnish urban district," *Energies (Basel)*, vol. 13, no. 10, May 2020, doi: 10.3390/en13102478.
[10] Stanica DI, Bachmann M, Kriegel M. Design and performance of a multi-level cascading district heating network with multiple prosumers and energy storage. Energy Rep. Oct. 2021;7:128–39. https://doi.org/10.1016/j.egyr.2021.08.163.
[11] Fischer D, Madani H. On heat pumps in smart grids: A review. Renew. Sustain. Energy Rev. 2017;70(April):342–57. https://doi.org/10.1016/j.rser.2016.11.182.
[12] Gross M, Karbasi B, Reiners T, Altieri L, Wagner HJ, Bertsch V. Implementing prosumers into heating networks. Energy Sep. 2021;230. https://doi.org/10.1016/j.energy.2021.120844.
[13] Brand L, Calvén A, Englund J, Landersjö H, Lauenburg P. Smart district heating networks - A simulation study of prosumers' impact on technical parameters in distribution networks. Appl. Energy 2014;129:39–48. https://doi.org/10.1016/j.apenergy.2014.04.079.
[14] M. H. Abokersh, K. Saikia, L. F. Cabeza, D. Boer, and M. Vallès, "Flexible heat pump integration to improve sustainable transition toward 4th generation district heating," *Energy Convers Manag*, vol. 225, no. May, 2020, doi: 10.1016/j.enconman.2020.113379.
[15] University of Wisconsin–Madison: Solar Energy Laboratory, "TRNSYS 17, a transient simulation program." Madison, Wis. : The Laboratory, 1975., 1975. Accessed: Oct. 05, 2023. [Online]. Available: https://www.trnsys.com/.
[16] Hmadi M, Mourtada A, Daou R. Forecasting the performance of a district solar thermal smart network in desert climate – A case study. Energy Convers Manag Mar. 2020;207. https://doi.org/10.1016/j.enconman.2020.112521.
[17] Calise F, Cappiello FL, Dentice d'Accadia M, Vicidomini M. Smart grid energy district based on the integration of electric vehicles and combined heat and power generation. Energy Convers Manag 2021;234:113932. https://doi.org/10.1016/j.enconman.2021.113932.
[18] Calise F, Cappiello FL, Dentice d'Accadia M, Petrakopoulou F, Vicidomini M. A solar-driven 5th generation district heating and cooling network with ground-source heat pumps: a thermo-economic analysis. Sustain. Cities Soc. 2022;76:Jan. https://doi.org/10.1016/j.scs.2021.103438.
[19] von Rhein J, Henze GP, Long N, Fu Y. Development of a topology analysis tool for fifth-generation district heating and cooling networks. Energy Convers Manag 2019;196(March):705–16. https://doi.org/10.1016/j.enconman.2019.05.066.
[20] M. Tunzi, M. Ruysschaert, S. Svendsen, and K. M. Smith, "Double loop network for combined heating and cooling in low heat density areas," *Energies (Basel)*, vol. 13, no. 22, 2020, doi: 10.3390/en13226091.
[21] Augusto GL, Culaba AB. "Identification of design criteria for district cooling distribution network with loop-type system", in Energy Procedia. Elsevier Ltd 2019:2132–8. https://doi.org/10.1016/j.egypro.2019.01.610.
[22] Eremin A, Trubitsyn K, Kolesnikov S, Kudinov I, Tkachev V. Computer models of hydraulic systems of district heating. MATEC Web of Conferences 2018;193:1–9. https://doi.org/10.1051/matecconf/201819302028.
[23] Yan A, Zhao J, An Q, Zhao Y, Li H, Huang YJ. Hydraulic performance of a new district heating systems with distributed variable speed pumps. Appl. Energy 2013;112:876–85. https://doi.org/10.1016/j.apenergy.2013.06.031.
[24] Wang H, Wang H, Zhu T. A new hydraulic regulation method on district heating system with distributed variable-speed pumps. Energy Convers Manag 2017;147:174–89. https://doi.org/10.1016/j.enconman.2017.03.059.
[25] Lickleder T, Hamacher T, Kramer M, Perić VS. Thermohydraulic model of Smart Thermal Grids with bidirectional power flow between prosumers. Energy 2021;230. https://doi.org/10.1016/j.energy.2021.120825.
[26] S.A. Klein *et al.*, *TRNSYS 17 - Mathematical Reference*. 2012. [Online]. Available: http://sel.me.wisc.edu/trnsys.
[27] Cengel Yunus and Cimbala John M., *Fluid Mechanics: Fundamentals and Applications*. 2014.
[28] Danielewicz J, Śniechowska B, Sayegh MA, Fidorów N, Jouhara H. Three-dimensional numerical model of heat losses from district heating network pre-insulated pipes buried in the ground. Energy 2016;108:172–84. https://doi.org/10.1016/j.energy.2015.07.012.
[29] Catrini P, Testasecca T, Buscemi A, Piacentino A. Exergoeconomics as a Cost-Accounting Method in Thermal Grids with the Presence of Renewable Energy Producers. Sustainability 2022;14(7):4004. https://doi.org/10.3390/su14074004.
[30] ASHRAE, *DISTRICT HEATING GUIDE - Complete Design Guide for District Heating Systems*. 2013. [Online]. Available: www.ashrae.org.
[31] G. Lennermo, P. Lauenburg, and L. Brand, "Decentralized heat supply in district heating systems - implications of varying differential pressure," *14th International Symposium on DH and Cooling*, p. 6, 2014, [Online]. Available: http://www.svenskfjarrvarme.se/Global/Konferenser/DHC14/Proceedings/_5.2 Gunnar Lennermo DECENTRALISED HEAT SUPPLY IN DISTRICT HEATING SYSTEMS IMPLICATIONS OF VARYING DIFFERENTIAL PRESSURE.pdf.
[32] DPR 26 agosto 1993, n. 412 - REGOLAMENTO RECANTE NORME PER LA PROGETTAZIONE, L'INSTALLAZIONE,L'ESERCIZIO E LA MANUTENZIONE DEGLI IMPIANTI TERMICI DEGLI EDIFICI AIFINI DEL CONTENIMENTO DEI CONSUMI DI ENERGIA, IN ATTUAZIONE DELL'ART.4, COMMA 4, DELLA LEGGE 9 GENNAIO 1991, N. 10.
[33] Piacentino A, Barbaro C. A comprehensive tool for efficient design and operation of polygeneration-based energy μgrids serving a cluster of buildings. Part II: Analysis of the applicative potential. Appl. Energy 2013;111:1222–38. https://doi.org/10.1016/j.apenergy.2012.11.079.
[34] "Energy Plus." [Online]. Available: https://energyplus.net/.
[35] U.S. Department of Energy, "Prototype Building Models." Accessed: Sep. 26, 2023. [Online]. Available: https://www.energycodes.gov/prototype-building-models.
[36] ASHRAE and American National Standards Institute, "Climatic Data for Building Design Standards," 2020. [Online]. Available: www.ashrae.org.
[37] EnergyPlus, "Weather Data by Location." Accessed: Oct. 05, 2023. [Online]. Available: https://energyplus.net/weather-location/europe_wmo_region_6/ITA/ITA_Palermo.164050_IWEC.
[38] Task Force Customer Installations, "Guidelines for District Heating Substations Approved by the Euroheat & Power Board Prepared by Task Force Customer Installations EUROHEAT & POWER Guidelines for District Heating Substations October 2008," *Euroheat and Power*, 2008.
[39] Tol HI, Svendsen S. Improving the dimensioning of piping networks and network layouts in low-energy district heating systems connected to low-energy buildings: A case study in Roskilde, Denmark. Energy 2012;38(1):276–90. https://doi.org/10.1016/j.energy.2011.12.002.
[40] Oppermann G, Arnold O, Ködel J, Büchler M, Jutzeler M, et al, "Teleriscaldamento, teleraffreddamento", vol, et al. 2020. Accessed: Sep. 24, 2023. [Online]. Available: https://www.aelsi.ch/documenti/31.pdf; 2018.
[41] F.-C. Software, "EES_manual.pdf," pp. 210–212, 2011.
[42] ISPRA, "Fattori di emissione atmosferica di gas a effetto serra nel settore elettrico nazionale e nei principali Paesi Europei," 2019.
[43] M. Steen, "Greenhouse gas emissions from fossil fuel fired power generation systems." [Online]. Available: http://www.jrc.nl.